

Interim Report For The Upper Mississippi River - Illinois Waterway System Navigation Study



US Army Corps
of Engineers

February 2000

Rock Island District
St. Louis District
St. Paul District

The contents of this report are not to be used for advertising, publication, or promotional purposes. Citation of trade names does not constitute an official endorsement or approval of the use of such commercial products.

The findings of this report are not to be construed as an official Department of the Army position, unless so designated by other authorized documents.



PRINTED ON RECYCLED PAPER

Shear Stress on Shallow-Draft Barge Hulls

by Stephen T. Maynard

U.S. Army Engineer Research and Development Center
3909 Halls Ferry Road
Vicksburg, MS 39180-6199

Interim report

Approved for public release; distribution is unlimited

Prepared for U.S. Army Engineer District, Rock Island
Rock Island, IL 61204-2004
U.S. Army Engineer District, St. Louis
St. Louis, MO 63103-2833
U.S. Army Engineer District, St. Paul
St. Paul, MN 55101-1638

Engineer Research and Development Center Cataloging-in-Publication Data

Contents

Preface	iv
1—Introduction.....	1
Background.....	1
Objective.....	1
2—Factors Affecting Flow beneath Vessels.....	2
3—Shear Stress Along Hull of Tows.....	3
General.....	3
Hydraulically Smooth Hull--Large Underkeel Clearance	4
Nonhydraulically Smooth Hull--Large Underkeel Clearance	6
Small Underkeel Clearance	9
Analysis of Couette Flow	16
Application to UMRS Tows	19
Channel Bottom Shear Stress beneath Tows	20
Flow Quantity between Hull and Channel Bottom.....	21
4—Discussion of Results and Conclusions	24
References.....	25

SF 298

Preface

The work reported herein was conducted as part of the Upper Mississippi River - Illinois Waterway (UMR-IWW) System Navigation Study. The information generated for this interim effort will be considered as part of the plan formulation process for the System Navigation Study.

The UMR-IWW System Navigation Study is being conducted by the U.S. Army Engineer Districts, Rock Island, St. Louis, and St. Paul, under the authority of Section 216 of the Flood Control Act of 1970. Commercial navigation traffic is increasing and, in consideration of existing system lock constraints, will result in traffic delays which will continue to grow into the future. The system navigation study scope is to examine the feasibility of navigation improvements to the Upper Mississippi River and Illinois Waterway to reduce delays to commercial navigation traffic. The study will determine the location and appropriate sequencing of potential navigation improvements on the system, prioritizing the improvements for the 50-year planning horizon from 2000 through 2050. The final product of the System Navigation Study is a Feasibility Report which is the decision document for processing to Congress.

The study was performed by members of the staff of the U.S. Army Engineer Research and Development Center (ERDC), Waterways Experiment Station (WES), Coastal and Hydraulics Laboratory (CHL), during 1997-1998. The study was under the direction of Dr. James R. Houston, Director, CHL; Mr. Charles C. Calhoun, Jr., Assistant Director, CHL; and Mr. C. E. Chatham, Jr., Chief, Navigation and Harbors Division (NHD), CHL. The study was conducted by Dr. S. T. Maynard, Navigation Branch, NHD.

At the time of publication of this report, Dr. Lewis E. Link was Acting Director of ERDC. COL Robin R. Cababa, EN, was Commander.

The contents of this report are not to be used for advertising, publication, or promotional purposes. Citation of trade names does not constitute an official endorsement or approval of the use of such commercial products.

1 Introduction

Background

The Upper Mississippi River-Illinois Waterway System (UMR-IWWS) Navigation (Feasibility) Study will evaluate the justification of providing additional lockage capacity at sites on the UMR-IWWS while maintaining the social and environmental qualities of the river system. The system navigation feasibility study will be accomplished by executing the Initial Project Management Plan (IPMP) outlined by the U.S. Army Engineer Districts (USAED), St. Paul, Rock Island, and St. Louis (1994). The IPMP outlines Engineering, Economic, Environmental, and Public Involvement Plans.

The Environmental Plan identifies the significant environmental resources on the UMR-IWWS and probable impacts in terms of threatened and endangered species, water quality, recreational resources, fisheries, mussels and other macroinvertebrates, waterfowl, aquatic and terrestrial macrophytes, and historic properties. It considers system-wide impacts of navigation capacity increases, while also assessing in preliminary fashion potential construction effects of improvement projects.

One element of the Environmental Plan addresses the impacts of navigation on larval and adult fish. Part of the fish study evaluates the impact of early life stages of fish passing near the hull of the vessel where they could be exposed to shear stress that could lead to mortality. The waterway zone passing adjacent to the hull, the distribution of larval fish in the hull passage zone, the quantity of water passing through the zone having lethal values of shear, and the mortality of larval fish under shear stress are all parts of the larval fish study.

Objective

This study is a component of the larval fish study, and the objective is to define the variation of shear stress in the zone between the hull of the tow and the channel bottom and to define the quantity of water in this zone for typical UMRS tows.

2 Factors Affecting Flow beneath Vessels

The flow patterns beneath the hull of a moving tow are quite complex, particularly with low underkeel clearance (UKC) and with ambient currents that are either against the tow (upbound tow) or with the tow (downbound tow). Return velocity is the flow created by the tow's motion and has a direction opposite to the direction of the tow. Return velocity increases with vessel speed relative to the water and decreases with increasing area of the cross section. In navigable rivers, low-flow periods generally result in low UKC, high return velocity, and low ambient velocities. Conversely, moderate- to high-flow periods result in large UKC, low return velocity, and high ambient velocities. The ambient flow conditions are often important because they can act in the same or opposite direction to the return flows.

In Maynard (1990), a near-bed displacement velocity was identified as the large peak in velocity acting opposite the direction of the tow just astern of the end of the rake near the bow of the tow in slack water conditions. The displacement velocity is caused by the contraction of flow at the rake of the lead barges and is relatively short lived. For barges having poorly formed rakes, separation at the bow could increase the displacement flow. Return velocity lasts for the duration of the passage of the tow.

Consider near-bed velocities beneath a downbound tow. The displacement velocity and the return velocity attempt to move flow upstream, the ambient velocity is downstream, and the shear along the hull is dragging water in a downstream direction. Unless the displacement velocity exceeds the ambient velocity, near-bed velocity will remain in a downstream direction near the bow of the tow. Unless the return velocity exceeds both the ambient velocity and the hull shear effects, near-bed velocity along the length of the vessel will remain in a downstream direction.

For an upbound tow, the displacement velocity and the return velocity attempt to move flow downstream, the ambient velocity is downstream, but the shear along the hull is dragging water in an upstream direction. Near-bed velocity beneath the upbound tow will generally be in a downstream direction except for low depth/draft ratios where the hull shear effects can dominate flow beneath the vessel and cause flow in an upstream direction.

3 Shear Stress Along Hull of Tows

General

When water flows past a solid boundary, the friction along the boundary retards the motion of the water next to the boundary. The zone of retarded flow is called the boundary layer. As shown in the Figure 1 schematic, the velocity in the boundary layer is zero at the boundary (hull) and the shear stress is a maximum at the boundary. The limit of the boundary layer is generally defined as the point where the velocity is equal to 0.99 times the velocity outside the boundary layer. At the limit of the boundary layer, the velocity is at a maximum and the shear stress is near zero. Since the boundary thickness grows with distance from the point of initiation, the amount of flow in the boundary layer increases with distance from the initiation point. The flow in a boundary layer of a vessel is turbulent except for a short distance near the bow. Turbulent flow along a hull is characterized by eddies having size ranging from minute to about the size of the boundary layer thickness. These eddies will thoroughly mix the boundary layer in a relatively short distance, which is on the order of 20 to 50 times the boundary layer thickness.

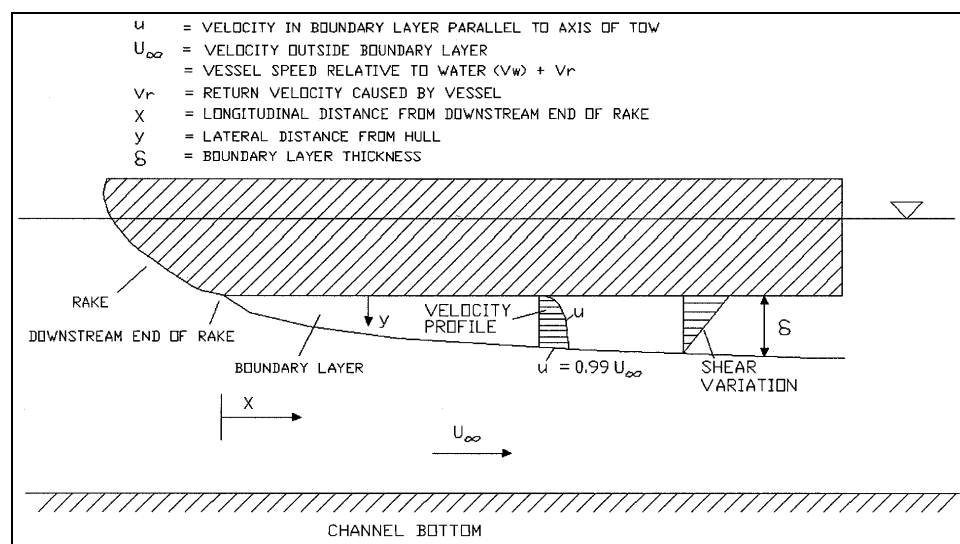


Figure 1. Schematic of boundary layer along hull of vessel

Boundary layer equations for flow in a developing boundary layer were used to determine the variation of shear with distance from the bow of the vessel and the variation with distance measured perpendicular to the hull. The analysis uses equations for zero pressure gradient which is standard in vessel resistance analysis. The analysis presented herein ignores the discontinuities at the junctions between barges. While these junctions certainly have some local effect, they do not eliminate the zone of retarded flow near the hull, and the analysis that follows uses a continuous hull surface. The ultimate objective is to compare the computed shear stress in the boundary layer near the hull with the lethal values of shear stress from Morgan et al. (1976) and additional mortality studies conducted as part of the UMR-IWWS studies. The following analysis will address both hydraulically smooth and rough hull assumptions.

Hydraulically Smooth Hull--Large Underkeel Clearance

The smooth boundary equations from Nikuradse (Schlichting 1968, p 605) were used because they are applicable to large Reynolds numbers. The equation from Schlichting for the velocity profile on a hydraulically smooth surface is

$$\frac{u}{U_{\infty}} = 0.737 \left(\frac{y}{d_1} \right)^{0.1315} \quad (1)$$

where

u = velocity at distance y away from the boundary

$U4$ = velocity outside the boundary layer and set equal to the vessel speed plus the computed return velocity

δ_1 = displacement thickness

Nikuradse found velocity profiles are similar and independent of Reynolds number when $u/U4$ is plotted against y/δ_1 . $U4$ is computed with the return velocity rather than the displacement velocity, because the displacement velocity acts over only a small portion of the vessel hull. A schematic is shown in Figure 1. The displacement thickness from Nikuradse is determined from

$$d_1 = 0.01738 R_x^{0.861} \frac{n}{U_{\infty}} \quad (2)$$

where

R_x = Reynolds number defined as $U4 x/\nu$

ν = kinematic viscosity of water

x = distance from the beginning of boundary layer development

The displacement thickness indicates the distance by which the external streamlines are shifted because of the formation of the boundary layer. The local friction coefficient c'_{fs} from Nikuradse is defined as

$$c'_{fs} = 0.02296 R_x^{-0.139} \quad (3)$$

The boundary shear stress τ is given by

$$t = 1/2 \rho c'_{fs} U_\infty^2 \quad (4)$$

where ρ is the water density.

Equation 4 can be used with smooth or rough hulls and the local skin friction coefficient to define the shear as a function of distance along the hull or with the total skin friction coefficient to define the average shear over the hull for either rough or smooth hulls. (Nikuradse also provides an equation similar to Equation 3 for the total skin friction coefficient on a smooth boundary.) If the boundary layer thickness δ is defined as the point at which the velocity in the boundary layer is 0.99 times the velocity outside the boundary layer, Equation 1 results in

$$d = 9,433 d_1 \quad (5)$$

Similar to an open channel, a linear variation of shear from the boundary to the limits of the boundary layer (δ) where shear is near zero is a fair approximation (Schlichting 1968, p 532). The discharge within the boundary layer or any portion of the boundary layer can be determined from integration of Equation 1 over y and substitution of Equation 5 resulting in

$$q = 0.87 \left(\frac{d}{d} \right)^{0.1315} d U_\infty \quad (6)$$

where

d = distance away from the boundary (must be less than δ) over which the discharge is to be determined

q = unit discharge within d

The total discharge Q over the hull is

$$Q = q (B + 2D) \quad (7)$$

where

B = vessel width

D = vessel draft

While the sides of the vessel do not have the effects of the channel bottom, both are treated the same because the flow patterns are similar.

A typical UMRS vessel with length of 297 m (975 ft) (5 barges long), beam of 32 m (105 ft) (3 barges wide), draft of 2.74 m (9 ft), waterway width of 305 m (1,000 ft), waterway area of 930 sq m (10,000 sq ft), and vessel speed of 3.05 m/sec (10.0 ft/sec) was used to evaluate the flow in the boundary layer. The computed return velocity for this tow is 0.58 m/sec (1.9 ft/sec), giving a $U/4$ of 3.6 m/sec (11.9 ft/sec). The boundary layer thickness and displacement thickness for the smooth hull assumption are shown in Figures 2 and 3, respectively. Boundary layer growth is assumed to begin at the downstream end of the rake because the contraction of the rake is assumed to inhibit the growth of the boundary layer. Note that the boundary layer thickness often reaches a magnitude that extends to the channel bottom. Past this point, these methods begin to lose their validity.

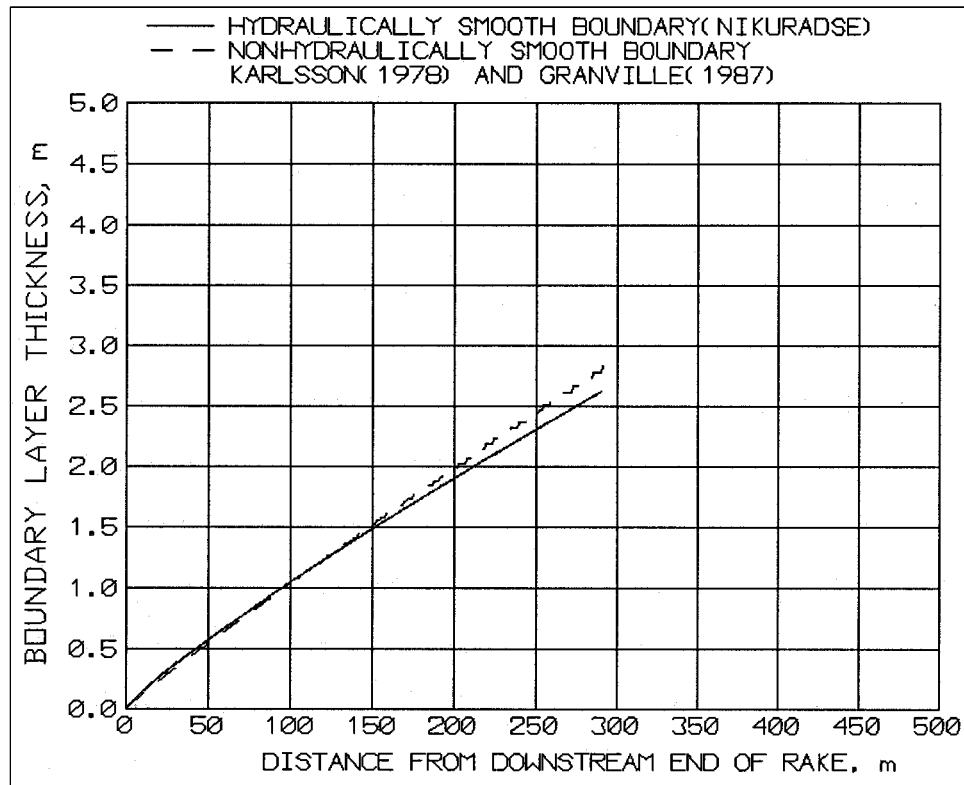


Figure 2. Boundary layer thickness versus distance from downstream end of rake, vessel speed relative to water = 3.63 m/sec

Nonhydraulically Smooth Hull--Large Underkeel Clearance

The assumption of a hydraulically smooth hull is generally not met on the hull of a barge but does represent a lower bound for the shear stress. Karlsson (1978) conducted resistance tests on four different surfaces typical of that found on vessels. Local skin friction was measured with the "floating element method" which involved measuring the drag on a small plate positioned at various points

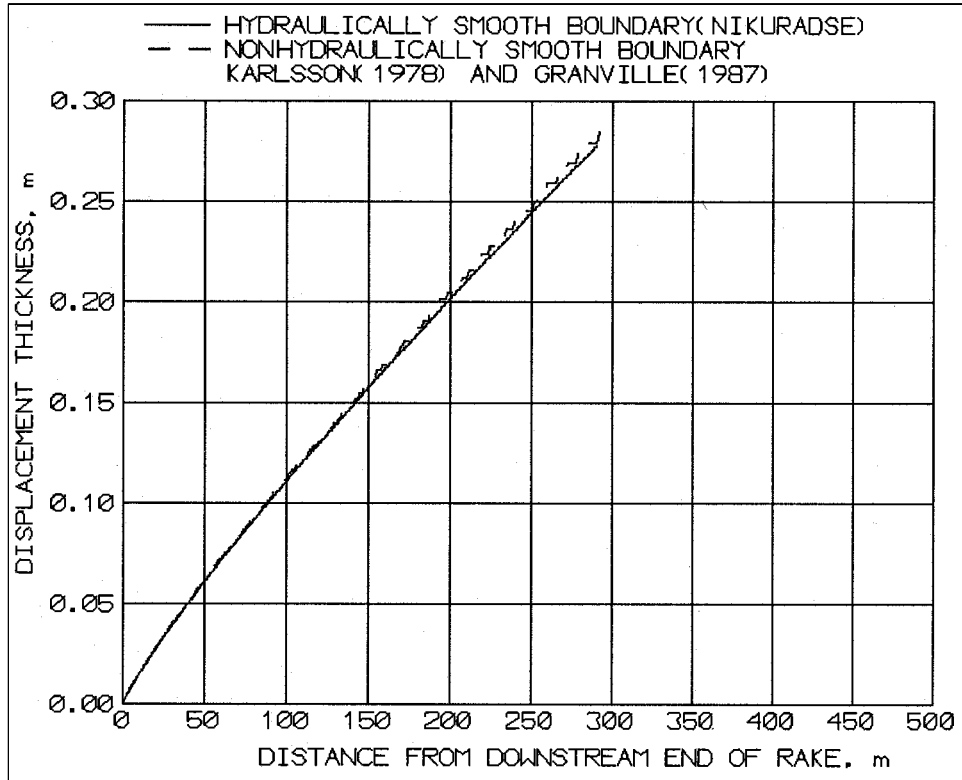


Figure 3. Displacement thickness versus distance from downstream end of rake, vessel speed relative to water = 3.63 m/sec

along the developing boundary layer. One of the four surfaces tested, surface 3, “is from an older ship and is probably painted without prior sandblasting.” Surface 3 was selected for the analysis herein because its high roughness represents a worst case in terms of boundary layer shear stress.

For surface 3, the downward shift of the logarithmic velocity distribution ΔB for $R_k > 17$ is

$$\Delta B = 2.44 \ln R_k - 3.05 \quad (8)$$

where

$$R_k = U_r^* k / \nu$$

$$U_r^* = \text{rough surface shear velocity} = (\tau/\rho)^{1/2}$$

Note that B is defined as width previously. ΔB is retained herein to be consistent with Karlsson (1978). Karlsson (1978) defined k as the root mean square value of the roughness height and was equal to 0.183 mm for surface 3. The limitation of $R_k > 17$ for surface 3 results in $\tau > 74$ dynes/sq cm which is exceeded for any typical UMR-IWWS vessel and speed based on measured and calculated shear presented later in this report. Karlsson gives the relationship of ΔB to the smooth surface shear velocity U_s^* and U_r^* as

$$\Delta B = \frac{U_\infty}{U_s^*} - \frac{U_\infty}{U_r^*} \quad (9)$$

Karlsson presents an equation from Coles (1953) to define the skin friction for smooth walls as

$$2 \left(\frac{U_s^*}{U_\infty} \right)^2 \left[\frac{U_\infty x}{n} + 2 \frac{C_1}{k^2} e^{-k\phi(1)} e^{k(C_2/C_1)} \right] = 2 C_1 e^{-k\phi(1)} e^{k(U_\infty/U_s^*)} \left[1 - \frac{U_s^*}{U_\infty} \left(\frac{2}{k} + \frac{C_2}{C_1} \right) + \frac{2}{k} \left(\frac{U_s^*}{U_\infty} \right)^2 \left(\frac{1}{k} + \frac{C_2}{C_1} \right) \right] \quad (10)$$

where the constants are defined as $C_1=4.05$, $C_2=29.0$, $\kappa=0.4$, and $\phi(1)=7.9$.

Equation 10 is solved for U_s^* by an iterative method and c'_{fs} is determined from Equation 4 with $\tau = (U_s^*/\rho)^{0.5}$. The hull shear for a smooth hull based on Equation 10 is shown in Figure 4 for the typical UMRS tow used in the boundary layer calculations above. The Figure 4 shear stress is nearly identical to values of shear stress obtained from Nikuradse's Equations 3 and 4.

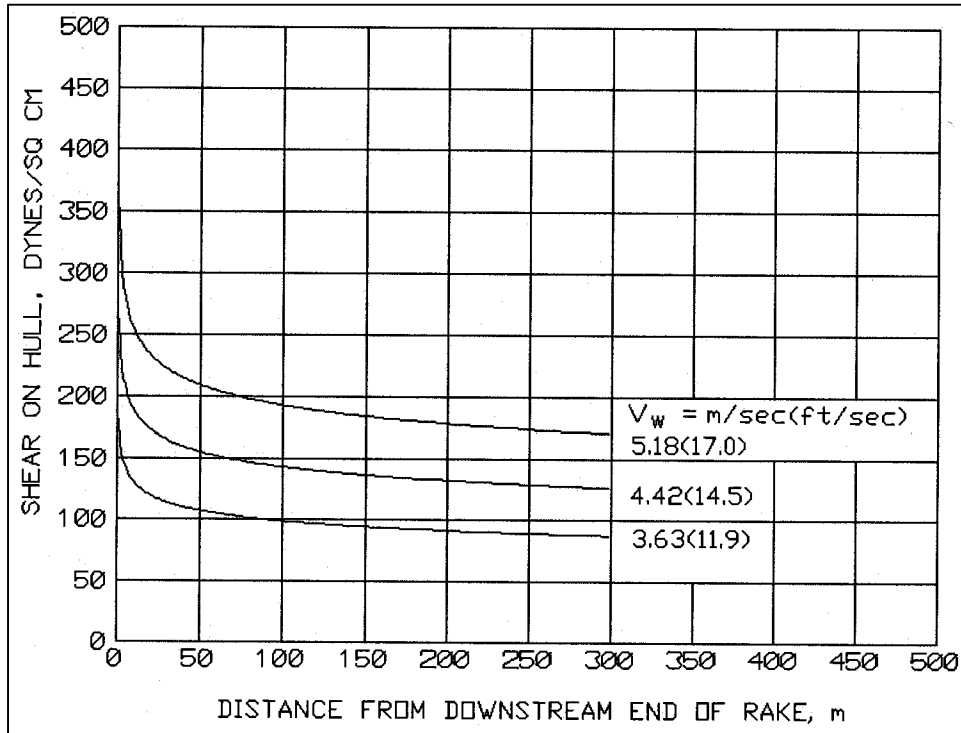


Figure 4. Shear on hull versus distance from downstream end of rake versus speed relative to water (equal to vessel speed plus return velocity), hydraulically smooth hull

Knowing U_s^* , U_4 , k , and v for each x allows determination of U_r^* by using Equations 8 and 9. The hull shear for the nonhydrodynamically smooth hull based on the Karlsson surface 3 is given in Figure 5. The nonsmooth hull shear for Karlsson's surface 3 is about one-third greater than the smooth hull shear.

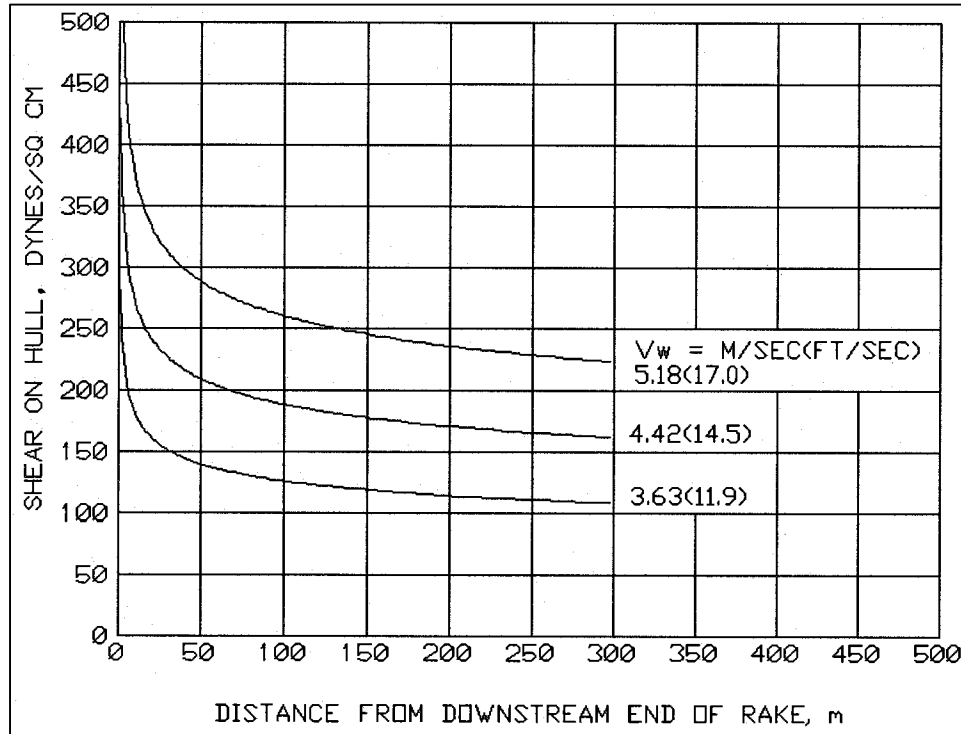


Figure 5. Shear on hull versus distance from downstream end of rake versus speed relative to water (equal to vessel speed plus return velocity), based on Karlsson (1978) for hulls that are not hydraulically smooth, Karlsson surface 3, $K = 0.183$ mm

Karlsson did not provide a method for calculating boundary layer or displacement thickness for the nonsmooth boundary. Using local skin friction coefficients based on the Karlsson equations for smooth and rough boundaries (surface 3), Granville (1987) was used to calculate the boundary layer thickness and displacement thickness as shown in Figures 2 and 3, respectively. Both thicknesses for the rough boundary differed little from the corresponding thicknesses for the smooth boundary.

Small Underkeel Clearance

As stated above, the boundary layer equations are not valid when the distance between hull and the channel bottom becomes less than the boundary layer thickness which is frequently the case on UMRS tows. UKC of as little as 0.6 m are common. One factor that will affect the hull shear and the number of larval fish passing through the shear zone is the small amount of flow that is actually

going under the vessel when UKC becomes small, because a large portion of the flow is diverted around the sides of the vessel.

To determine hull shear for the condition of low UKC, physical model experiments were conducted in the Navigation Effects Flume shown in Figure 6. Hull shear was measured using hot film anemometers mounted in the plexiglas barge as shown in Figure 7. The removable rake shown in Figure 7 was attached to the lead barge. The model tow was constructed from five of the plexiglas barges shown in Figure 7. The draft was 0.098 m except for one test that had a 0.028-m draft. The position of the two hot film gauges was changed by positioning the barge having the gauges at the bow of the tow, the middle, and at the stern. The cross section used in the middle 61 m of the Navigation Effects Flume is shown in Figure 8 (prototype dimensions are shown based on a scale ratio of 1:25) and was constructed of plastic-coated plywood. The hot film anemometers were calibrated in a 1.27-cm by 22.86-cm rectangular plexiglas duct with a length of 4.6 m. Pressure taps along the length of the duct established the pressure gradient which was used to compute the shear stress. The calibration duct had turbulent flow and a usable calibration range of 2 to 47 dynes/sq cm.

Unless noted, all quantities regarding the physical model in this section are presented in model dimensions. The approach used herein is to determine the ratio of local friction coefficient measured in the model for low depth/draft to local friction coefficient computed using the equation for a smooth flat plate. Since viscous forces are significant, the ratio must be determined using model quantities for both parameters. This local friction coefficient ratio will then be used to modify friction coefficients determined using flat plate equations and prototype dimensions. Results from the hull shear experiments are shown in Tables 1 through 3.

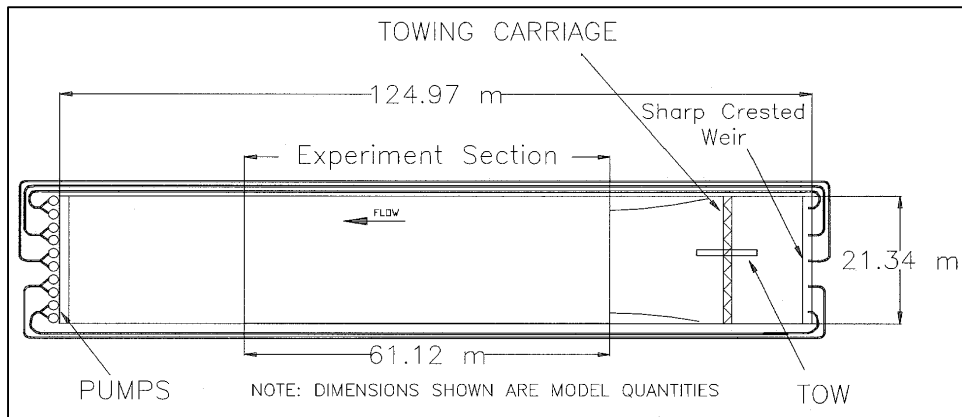


Figure 6. Navigation effects flume

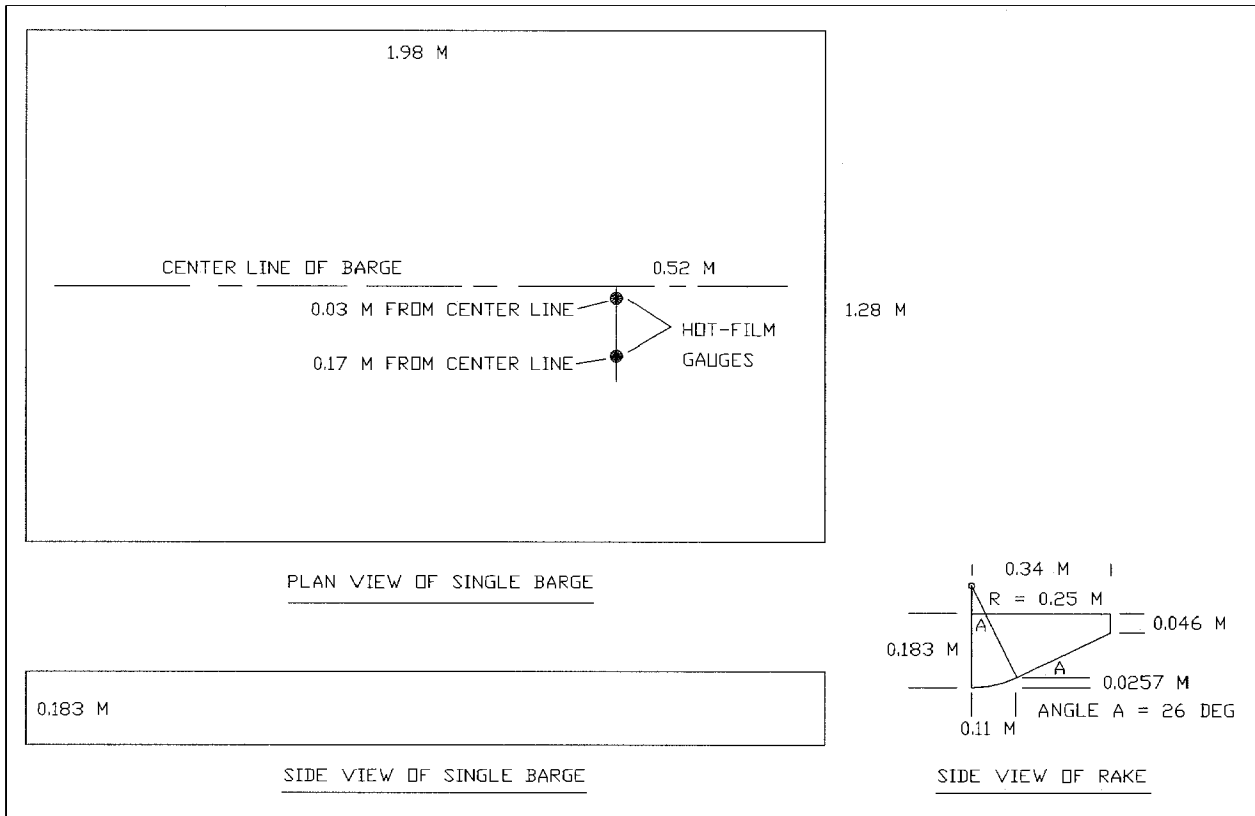


Figure 7. Hot-film gauge locations and barge dimensions

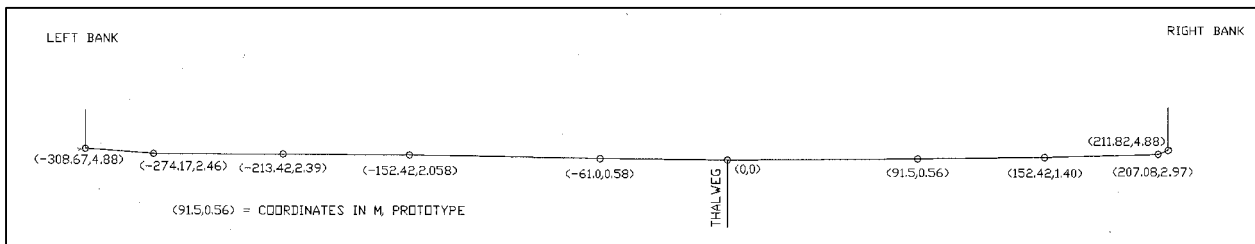


Figure 8. Cross section in experimental section, dimensions expressed as prototype equivalent of 1:25 scale model

Table 1
Measured Shear at 0.52 m from End of Rake

Depth, m	Draft, m	Depth/ Draft	Shear ¹ at Gauge 1, Gauge 2 in dynes/cm ²			
			V _g = 0.366 m/sec	0.548 m/sec	0.610 m/sec	0.854 m/sec
0.364	0.028	13.0	3.8,3.6	-	10.5,10.0	16.5,13.4
0.364	0.098	3.71	3.3,2.7	-	9.7,8.2	15.9,12.9
0.292	0.098	2.98	4.3,4.5	-	10.3,10.8	22.0,18.8
0.220	0.098	2.24	4.7,4.8	-	10.5,10.9	20.5,17.1
0.172	0.098	1.76	6.0,5.5	-	12.7,10.9	²
0.136	0.098	1.39	9.1,6.3	14.1,11.3	²	²

¹ Average of three replicates at each gauge.
² Vessel speed greater than limiting speed.

Table 2
Measured Shear at 4.48 m from End of Rake

Depth, m	Draft, m	Depth/ Draft	Shear ¹ at Gauge 1, Gauge 2 in dynes/cm ²			
			V _g = 0.366 m/sec	0.548 m/sec	0.610 m/sec	0.854 m/sec
0.364	0.028	13.0	3.7,4.0	-	7.5,8.5	10.5,9.4
0.364	0.098	3.71	2.8,2.5	-	9.3,6.9	12.9,10.7
0.292	0.098	2.98	1.5,2.3	-	8.0,7.0	16.4,12.3
0.220	0.098	2.24	3.0,2.6	-	9.8,7.3	16.2,13.4
0.172	0.098	1.76	4.7,3.6	-	10.8,8.5	²
0.136	0.098	1.39	4.0,3.2	7.6,7.2	²	²

¹ Average of three replicates at each gauge.
² Vessel speed greater than limiting speed.

Table 3
Measured Shear at 8.4 m from End of Rake

Depth, m	Draft, m	Depth/ Draft	Shear ¹ at Gauge 1, Gauge 2 in dynes/cm ²			
			V _g =0.366 m/sec	0.548 m/sec	0.610 m/sec	0.854 m/sec
0.364	0.028	13.0	1.8,1.9	-	5.4,5.2	10.7,10.4
0.364	0.098	3.71	6.9,2.4	-	7.4,6.3	15.2,11.2
0.292	0.098	2.98	2.2,2.6	-	6.6,6.1	10.9,10.8
0.220	0.098	2.24	2.9,3.1	-	6.9,7.7	14.3,13.9
0.172	0.098	1.76	2.6,2.3	-	6.9,6.7	²
0.136	0.098	1.39	1.8,1.5	4.4,3.6	²	²

¹Average of three replicates at each gauge.
²Vessel speed greater than limiting speed.

Hot film anemometry can be difficult in an environment like the Navigation Effects Flume which is exposed to dust and dirt blowing into the flume and has uncontrolled temperature. Considering these difficulties, the two gauges give relatively similar results. The shear from the two gauges was averaged and the local friction coefficient c'_{fs} was computed using Equation 4 with U_4 equal to vessel speed plus return velocity (average over the entire cross section) computed from Maynard (1996). For depth/draft of 13.0 and 3.71, c'_{fs} is plotted against R_x in Figure 9 along with the Nikuradse smooth boundary equation given by Equation 3. The two highest depth-over-draft ratios were used because they would be least influenced by the channel bottom and most likely to fit the standard boundary layer equations. The agreement between the shear from the experiments where the hull is far from the bottom and the Nikuradse Equation 3 is good. The observed values average about 15 percent greater than the smooth curve which is likely the result of the joints between barges, the difference between the shape of the barge rake and the entrance shape of a flat plate, and typical deviations with hot film anemometry. The c'_{fs} from Equation 3 was used to normalize all c'_{fs} determined using the measured shear stress, and this ratio is plotted versus depth/draft ratio in Figures 10 through 12 for each location along the tow. Depth/draft = 13.0 was not plotted because Figures 10 through 12 focused on the depth/drafts where low UKC is expected to cause increased shear stress. In the zone near the bow of the tow (0.52 m from end of rake), the hull shear increases significantly with decreasing depth/draft as shown in Figure 10. The best fit line in Figure 10 is given by

$$\frac{c'_{fs}}{c'_{fs}(\text{Nikuradse})} = 1.98 - 0.22 \frac{\text{Depth}}{\text{Draft}} \quad (11)$$

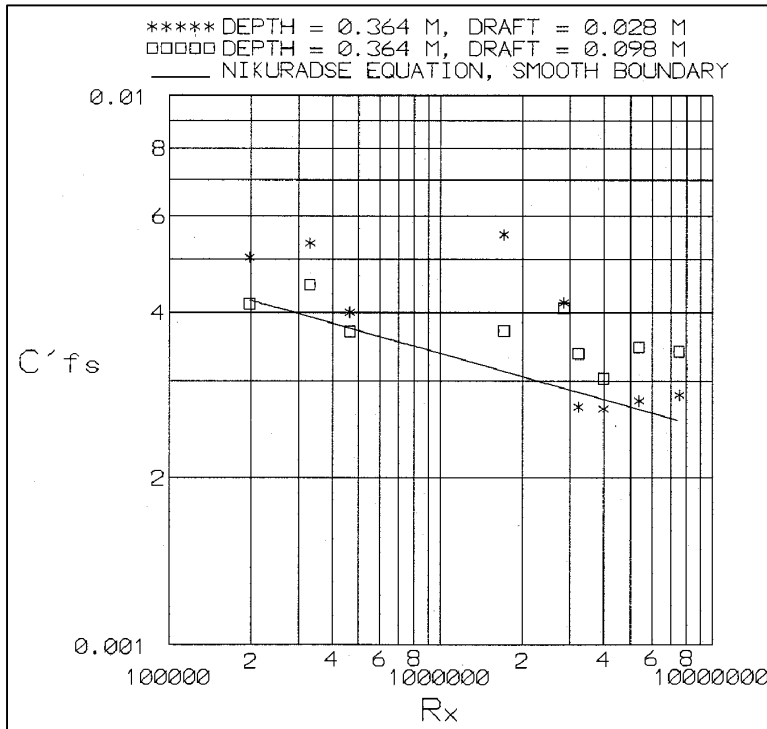


Figure 9. Local friction coefficient versus Reynold's number

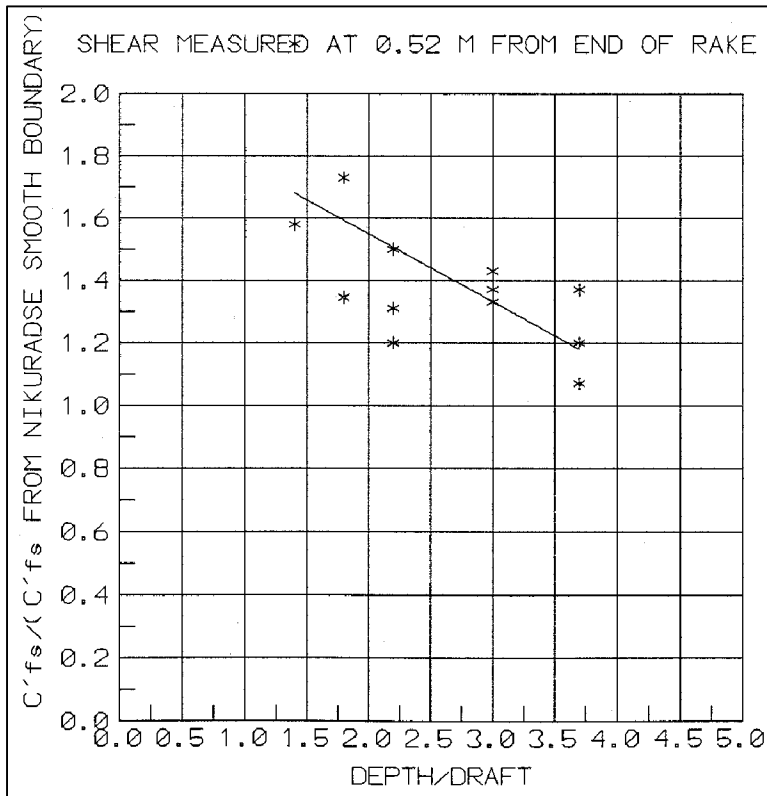


Figure 10. Friction coefficient ratio versus depth/draft, 0.52 m from end of rake

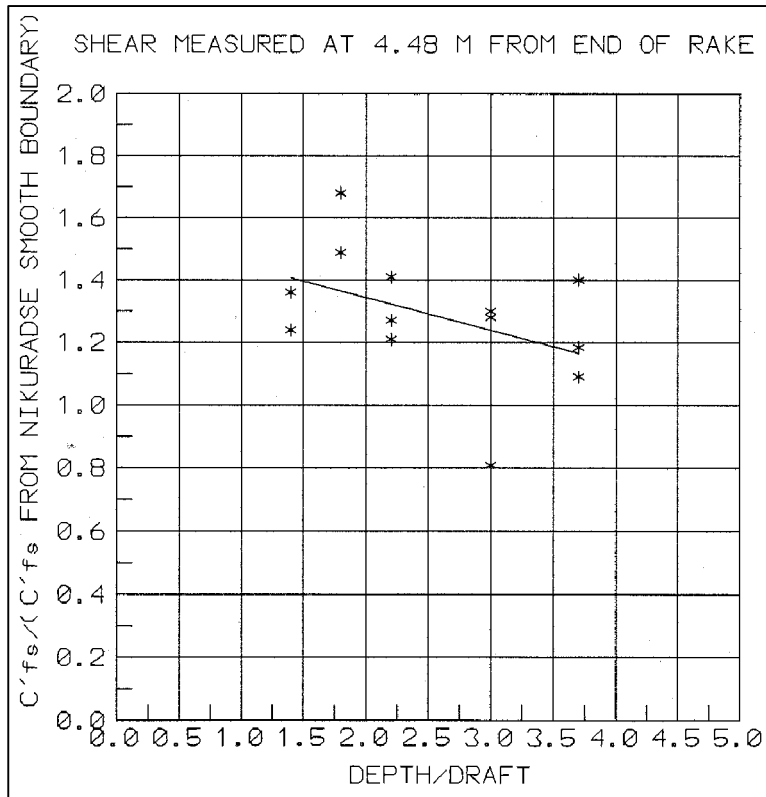


Figure 11. Friction coefficient ratio versus depth/draft, 4.48 m from end of rake

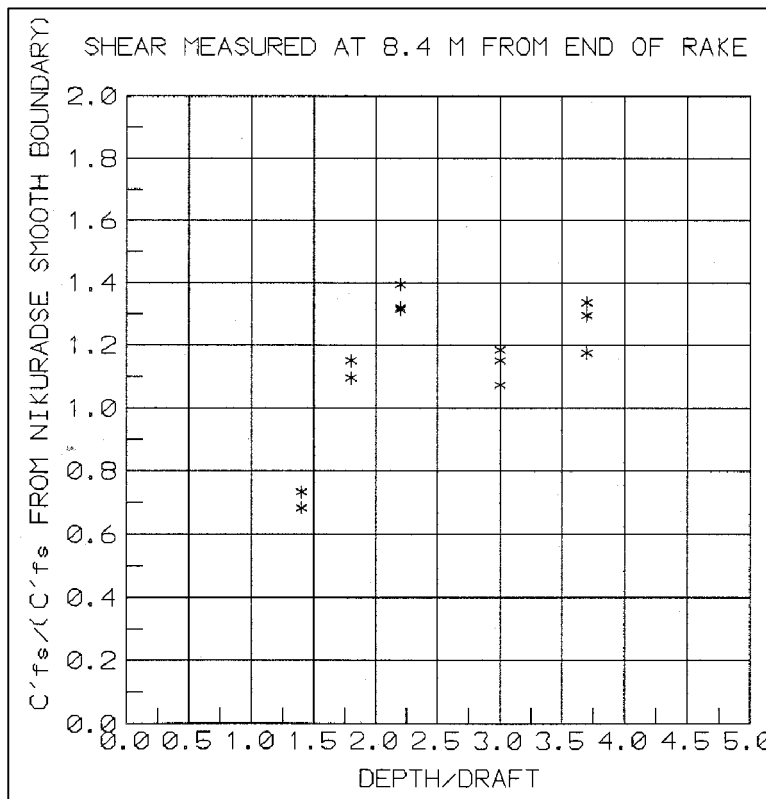


Figure 12. Friction coefficient ratio versus depth/draft, 8.4 m from end of rake

The right hand side of Equation 11 is a minimum of 1.0. Since the physical model is scaled on UMR-IWWS tows at a scale ratio of 1:25, Equation 11 is applicable to a point on the full-scale vessel hull $25(0.52) = 13$ m from the end of the rake.

In the zone near the middle of the tow (4.48 m from end of rake), the hull shear also increases, but at a lesser rate than at the bow, as shown in Figure 11. The best fit line description is

$$\frac{c'_{fs}}{c'_{fs}(\text{Nikuradse})} = 1.55 - 0.105 \frac{\text{Depth}}{\text{Draft}} \quad (12)$$

and is also limited to a minimum value of 1.0. Equation 12 is applicable to a point on the hull of the full size vessel at $25(4.48) = 112$ m from the end of the rake.

Near the stern of the tow (8.4 m from end of rake in the model or $25(8.4) = 210$ m in the full size tow), the shear shows no significant change until a decrease at depth/draft less than 1.8 as shown in Figure 12. This decrease is possibly the result of flow being forced from beneath the vessel by the low UKC or the flow approaching an equilibrium close to a Couette flow where the shear on the channel bottom and the hull are close to equal.

The lowest depth/draft used in the hull shear experiments was 1.39, which is greater than low water conditions which can have depth = 3.35 m and draft = 2.74 m or a depth/draft = 1.22. Values of depth/draft less than 1.39 were not used because of physical model floor irregularities which resulted in groundings of the model tow. In addition, as discussed under scale effects by Maynard and Martin (1997), the boundary layer is relatively larger in the physical model than in the prototype. Because the boundary layer begins development at the bow, the effective draft at the bow will be equal to the actual draft in the model. At the stern the difference between boundary layer effects (quantified by the difference in displacement thickness) in model and prototype will be about 0.012 m in the model and 0.30 m in the prototype. The effective draft at the stern in the model becomes $0.098 + 0.012$ m = 0.11 m using the largest model draft in Tables 1 through 3. In the prototype, this corresponds to a 2.75-m draft which is typical of loaded UMR-IWWS tows. The actual draft of 0.098 m (model) or 2.44 m (prototype) is used herein to provide some conservatism. Application of Equations 11 and 12 to depth/draft of 1.22 requires only a modest extrapolation of the data which ranges from 3.7 to 1.39 for loaded tows. Tables 1 through 3 show three conditions which are labeled “vessel speed greater than limiting speed.” This was true for the channel size and model tow used in the physical model experiments but Equations 11 and 12 are applicable to any low-flow beam, draft, vessel speed, and depth combination occurring on the UMR-IWWS.

Analysis of Couette Flow

Because of the geometric similarity of small UKC beneath a 250- to 300-m-long tow to Couette flow and after comments by one of the reviewers, the flow

beneath the vessel was evaluated to see if the analogy of Couette flow would provide a useful analysis tool. For the model barges having a total length of 10.24 m and a clearance of (depth = 0.136 m) - (draft = 0.098 m) = 0.074 m, the length/clearance ratio of $10.24/0.038 = 269$ makes it very tempting to assume fully developed flow in the small gap, since pipe flows become fully developed after a length of 20 to 40 pipe diameters. The length/clearance ratio for some tows on the river can be up to 500. In pipe flow, the flow is caused by the pressure gradient along the pipe and flow development only requires a rearrangement of the velocity profile by the boundary roughness. In Couette flow, the flow is caused by the motion of one boundary relative to the other and the distance required to develop Couette is not analogous to, and is greater than, the distance required to develop pipe flow. Complicating and maybe even dominating the lack of formation of Couette flow beneath a tow is the influence of return currents which acts opposite to the direction of travel of the tow. If fully developed Couette flow exists beneath the tow, all velocities relative to the bed between the bed and hull will be in the direction of tow travel. Return velocity relative to the bed acts in a direction opposite to tow travel and will slow down or prevent the formation of developed Couette flow. To check this hypothesis that Couette flow does not have the required length to form and/or that return currents inhibit formation of Couette flow, physical model measurements of shear stress were compared on the hull and on the bed. If Couette flow exists, the shear values should be similar in magnitude. Bed shear stress measurements in the Navigation Effects Flume were measured, as shown in Table 4, along with values from Tables 2 and 3 (Maynard in preparation). Results show that the shear is not equal on bed and hull and Couette flow has not yet formed for the conditions shown. The shallowest depth for which hull shear measurements were made, 0.136 m, shows hull shear approaching bed shear near the stern, suggesting that Couette flow conditions are being approached. As an additional check, the shear stress was calculated between the hull and bed, assuming the Couette flow for the hull shear experiment had a 0.136-m depth and using a velocity of 0.4 m/sec to compare to Table 4. For Couette flow conditions, the velocity at midway between the hull and bed, relative to the hull or relative to the bed, will be one-half the vessel speed relative to the ground. Using the logarithmic velocity distribution for a smooth boundary with $y = 1/2$ of the clearance = 0.019 m, velocity = $1/2$ of the ground speed = $1/2(0.4) = 0.2$ m/sec, and $\nu = 0.000001$ m²/sec, the computed shear for Couette flow conditions is 1.1 dynes/sq cm. Using Couette flow equations for rotating concentric cylinders from Lathrop, Fineberg, and Swinney (1992) and substituting vessel speed for cylinder rotation speed and clearance for gap width between cylinders, the computed shear beneath the model tow is 1.4 dynes/sq cm. The computed Couette flow shear values are less than measured on the hull showing that Couette flow conditions have not been achieved. The Couette flow analogy does not provide a useful analysis tool, because Couette flow has not formed for most tows on the river. Even for the lowest clearances on the river where Couette flow may form near the stern, the analogy is not useful because the highest shear stresses having potential for mortality are located forward, where Couette flow conditions have not formed.

Table 4 Bed and Hull Shear Stress Comparison(given in model quantities)					
Barge draft, m	Depth, m, and Speed, m/sec, in Bed Shear Experiments, m	Depth, m, and Speed, m/sec, in Hull Shear Experiments, m	Bed Shear beneath Barges,¹ dynes/sq cm	Hull Shear, dynes/sq cm	
				4.48 m	8.4 m
0.098	0.146, 0.4	0.136, 0.4	≈1 ²	4.3 ³	2.1 ³
0.098	0.183, 0.6	0.172, 0.61	≈1 ²	9.7	6.8

¹ Bed shear beneath barges was relatively constant after passage of the sharp peak at the bow.
² This value is approximate, because shear this low is below the range in the calibration facility.
³ Interpolated from Tables 2 and 3.

The correction ratios given by Equations 11 and 12 are based on hydraulically smooth boundaries in a 1:25 scale model where viscous forces are significant. These ratios are proposed for use in the prototype where viscous forces are generally insignificant. By using ratios rather than scaling up model values to prototype values, we avoid many of the problems with viscous forces in the model being larger than the prototype. But are these ratios affected by the viscous forces in the model to the extent that they would be significantly different if determined in the prototype? The mechanisms causing hull shear to increase because of low UKC is a steeper velocity gradient at the hull and/or increased turbulence near the hull because of the presence of the channel bottom. The lack of significant shear on the channel bottom presented in Table 4 suggests that turbulent fluctuations emanating from the bed and causing increased shear stress is not a major factor. The remaining factor, a steeper velocity gradient because of the confining effects of the channel bottom, will have some scale effects in a 1:25 Froude model because of the excess viscous forces. The differences because of excess viscous forces in the model are insignificant at the bow of the tow and much larger near the stern. Since Equations 11 and 12 are based on conditions near the bow and near the middle of the barges, they are based on data taken away from the stern where scale effects are most significant, and Equations 11 and 12 should not be strongly affected by scale effects. These correction ratios are simplifications of a complex problem that can only be fully addressed with a hydrodynamic model that incorporates a moving vessel, free surface effects, nonhydrostatic pressure, and channel geometries having low UKC. To the author's knowledge, ship hydrodynamicists have not developed such a model that has been verified with observed data. Lacking such a model, these ratios are recommended for determining the shear increase that occurs for nonsmooth, prototype hulls having low UKC.

Application to UMRS Tows

The following application demonstrates how these model-derived ratios are used to adjust prototype shear for low UKC as follows:

- a. Compute shear for smooth surface using Equation 3 for the desired vessel speed and length.
- b. Increase smooth surface shear equation by one-third to represent the Karlsson surface 3 rough surface. (Alternatively, the first two steps could be replaced by solving Equations 8 through 10 for surfaces other than Karlsson's surface 3.)
- c. Use ratios from Equations 11 and 12 to determine shear increase for low UKC. Note that this step provides the shear and the local skin friction coefficient at two points along the hull, one near the bow and one near midship.
- d. Use the local skin friction coefficient at these two points to determine an equation having the form of Equation 3 that applies to the entire length of the hull. This equation will only be applicable to the selected vessel speed and length.

These steps are used in the following example.

Consider Karlsson's surface 3 which is adopted herein as representative of UMR-IWWS barge hulls. Hull shear for Karlsson's surface 3 can be determined approximately using a 33-percent increase of the smooth hull Equation 3 or

$$c'_{fr} = 0.031 R_x^{-0.139} \quad (13)$$

For a typical vessel speed relative to water on the UMR-IWWS of 3.63 m/sec, Equation 13 is within 5 percent of the Karlsson equations except near the initial 3 m from the end of the rake. Equation 13 is used herein because of its much simpler nature, but note that Equation 13 is only applicable to Karlsson's surface 3. Let $V_w = 3.63$ m/sec (11.9 ft/sec) and UKC = 0.61 m with a vessel having a 2.74-m draft resulting in a depth/draft ratio = 1.22. While the minimum depth/draft ratio used in the experiments reported herein was 1.39, this represents the best available method and is used for lesser ratios.

- a. *First point near bow(Eq 11)*: At $x = 13$ m from the end of the rake, $R_x = 4.72(10)^7$ and c'_{fr} from Equation 13 = 0.00266. Using Equation 11, which is applicable to $x = 13$ m, results in a ratio of 1.72 and c'_{fr} @depth/draft ratio of 1.22 = $1.72(0.00266) = 0.00458$.
- b. *Second point near midship(Eq 12)*: At $x = 112$ m from the end of the rake, $R_x = 4.07(10)^8$ and c'_{fr} from Equation 13 = 0.00197. Using Equation 12, which is applicable to $x = 112$ m, results in a ratio of 1.42 and c'_{fr} @depth/draft ratio of 1.22 = $1.42(0.00197) = 0.00280$.

These two points provide two c'_{fr} and their respective R_x that define the equation

$$c'_{fr} \text{ at depth / draft ratio of } 1.22 = 0.259 R_x^{-0.228} \quad (14)$$

Note that this equation is only applicable to the selected vessel speed and length and Karlsson's surface 3. The same analysis produced the following equation for depth/draft ratio of 2.0

$$c'_{fr} \text{ at depth / draft ratio of } 2.0 = 0.159 R_x^{-0.206} \quad (15)$$

Equations 14 and 15 are based on the points at 13 m and 112 m rather than at 210 m, because the shear is highest near the bow of the vessel and this approach provides a conservative estimate at 210 m. Hull shear for depth/draft ratios of 2.0 and 1.22 are shown in Figure 13 for a vessel speed of 3.63 m/sec and Karlsson's surface 3. Figure 5 is recommended for depth/draft of 5.0 or greater. Figures 5 and 13 are the recommended hull shear results for typical tows on the UMR-IWWS.

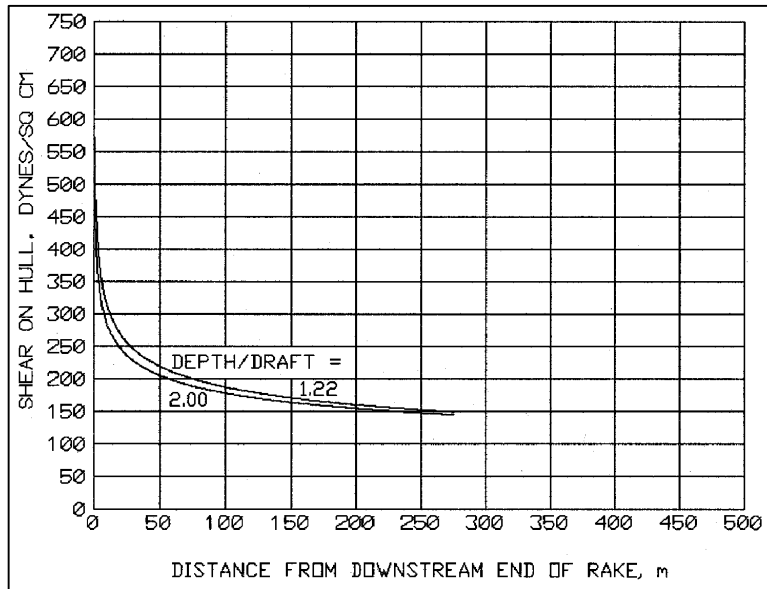


Figure 13. Shear on hull versus distance from downstream end of rake, based on Karlsson (1978) for hulls that are not hydraulically smooth, Karlsson surface 3, $K = 0.183$ mm, $V_w = 3.63$ m/sec

Channel Bottom Shear Stress beneath Tows

The dominant channel bottom shear stress beneath the hull of a vessel is located at the rapid velocity change near the bow as the displacement velocity builds to a peak. This peak in shear stress is also accompanied by a rapid decrease in pressure. The magnitude of these effects increase with decreasing depth/draft. Just astern of this peak, the bed shear stress depends on the net velocity from the

return velocity, the ambient velocity, and the hull shear dragging flow in the same direction as the tow. Physical model experiments were conducted in the Navigation Effects Flume to measure the shear stress on the channel bottom and are reported by Maynard (technical report in preparation).

Flow Quantity between Hull and Channel Bottom

The quantity of flow in the zone between the hull and the channel bottom must be defined. Equations 6 and 7 are recommended for UKC greater than 5.0. The following experiments provide a method for UKC < 5.0.

Physical model experiments were conducted to define the zone that passes under the hull of the vessel using dye injections at various distances from the tow center line (CL). The experiments were conducted in the previously described Navigation Effects Flume at a scale of 1:25. In this section of the report, all dimensions are expressed in their prototype equivalent. The model tow consisted of barges having the same dimensions as in the hull shear experiments. All experiments were conducted with a draft of 2.44 m. As stated in the previous section “Small Underkeel Clearance,” the effective draft at the stern is about equal to the commonly found loaded draft of 2.74 m. The actual draft of 2.44 m was used in the data analysis of this section to ensure some conservatism. The experiments were conducted with ambient currents and the inflow zone was determined for both upbound and downbound tows. The dye was injected on the channel bottom and spread laterally and vertically prior to arrival of the tow. The tow was passed through the dye cloud and the injection point location at which the center of the dye cloud passed along the edge of the barges was recorded. Results are shown in Table 5.

Depth, m	Tow Speed Relative to Ground, m/sec	Ambient Velocity, m/sec	Direction, Up or Down	Distance from Tow CL to Edge of Inflow Zone, m
3.35	1.83,2.74	0.6	Up	4.8
3.35	2.74,3.0	0.6	Down	5.7
4.0	2.74	0.55	Up	5.1
5.5	2.74	0.45	Up	7.6
5.5	3.66	0.45	Down	10.8
7.3	2.74	0.35	Up	10.5
7.3	2.74	0.35	Down	12.4

Figure 14 presents the percent of flow passing under the barges as a function of depth/draft. The flow passing under the barges is determined by doubling the distance from the last column of Table 5 and multiplying this distance by the depth and then by the vessel speed. For example, an upbound vessel traveling at 3.0 m/sec relative to a 3.35-m depth of water has a discharge passing between the hull and the channel bottom of $(4.8)(2)(3.0)(3.35) = 96 \text{ m}^3/\text{sec}$. The percent shown in Figure 14 is flow under the barges described above divided by the flow being intercepted by the barges defined as $(\text{beam}) \cdot (\text{depth}) \cdot (\text{vessel speed relative to water})$. In equation form, the flow beneath the vessel is defined as

$$Q(\text{beneath hull, low UKC}) = F_{pc} V_w B \text{Depth} \quad (16)$$

where F_{pc} is the percent of flow under the barge hull and is given by Figure 14.

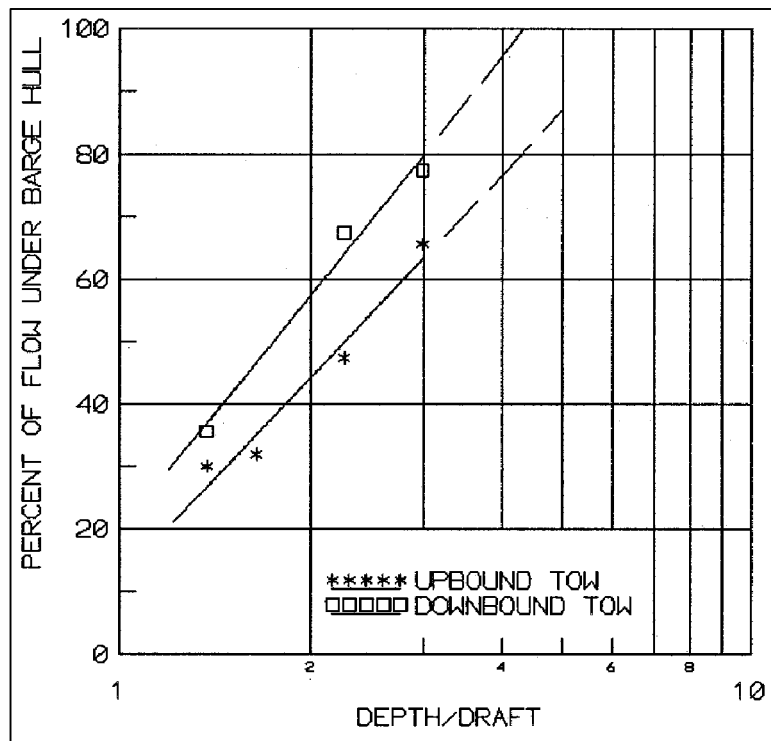


Figure 14. Percent of flow under barges versus depth/draft

Figure 14 is only applicable to UMR-IWW tow configurations and the typical speeds shown in Table 5. To apply the results in Figure 14 to the minimum depths and maximum drafts found on the UMR-IWW requires a small amount of extrapolation from depth/draft = $3.35/2.44 = 1.37$ (minimum used in experiments) to depth/draft = $3.35/2.74 = 1.22$ (minimum on UMR-IWWS). Since the curves on Figure 14 must go to $F_{pc} = 0$ at depth/draft = 1 and the effective draft is larger than 2.44 m over most of the tow, the extrapolation in Figure 14 will be conservative. The alternative to this approximate procedure was to measure detailed velocity profiles beneath the vessel and integrate the velocity over the area beneath the hull to define the discharge. This approach was not adopted because it could not be used for the shallowest of depths because of the physical size of the

velocity meter and because the measurements would have been quite difficult. This analysis treats the flow beneath the hull as a constant which is not the case for certain conditions. The dye streak beneath the barges after passage of the end of the rake remained parallel to the vessel and in a downstream direction for all downbound experiments, thus indicating that flow was not leaving the zone beneath the hull. For a 3.35-m depth and an upbound tow, the dye streak showed flow leaving the zone beneath the hull. The angle of the dye streak away from the tow center line increased with increasing distance from the bow. For evaluating larval fish mortality, the flow quantity is assumed to remain constant along the length of the barges.

In another UMR-IWWS report (Maynord in preparation), the author defined the zone of inflow to the propellers for the purpose of defining which region of the waterway was subject to passage through the propellers of a typical UMR-IWWS towboat. That report concluded that just ahead of the tow, a width of 25 m on either side of the center line of the tow could go through the propellers, but it did not state that all of the flow in that zone went through the propellers. Mixing between the bow and stern caused this zone to be wider than the zone defined herein. To assess the effects of tow traffic, biologists defined the concentration of larval fish and eggs in the 50-m-wide zone that was subject to passage through the propellers. A separate set of equations defined the quantity of flow through the propellers. The equations presented herein are used to determine the quantity of flow that will go through the hull shear zone and the width ranges from 10 to 25 m, depending on depth.

4 Discussion of Results and Conclusions

Flat plate shear equations and physical model experiments were used to determine hull shear beneath shallow-draft barge hulls. Results presented in Figures 5 and 13 quantify the hull shear for nonsmooth barge hulls in deep water and where UKC is as low as 0.6 m, which is common on the UMRS. Low UKC of about 0.6 m results in hull shear up to 50 percent greater than deep water hull shear.

Discharge between the hull and the channel bottom increases with increasing UKC or depth/draft.

Hull shear and quantity of flow between the hull and the channel bottom provide two of the needed parameters to compare to the shear causing mortality in larval fish. The third parameter, channel bottom shear, is provided by Maynard (in preparation).

References

- Coles, D. (1953). "Measurements in the boundary layer on a smooth flat plate in supersonic flow 1. The problem of the turbulent boundary layer," Report No. 20-69, Jet Propulsion Laboratory, California Institute of Technology, Pasadena, CA.
- Granville, P. S. (1987). "Three indirect methods for the drag characterization of arbitrarily rough surfaces on flat plates," *Journal of Ship Research* 31(1), 70-77.
- Karlsson, R. I. (1978). "The effect of irregular surface roughness on the frictional resistance of ships," *International Symposium on Ship Viscous Resistance*, SSPA, Goteborg.
- Lathrop, D. P., Fineberg, J., and Swinney, H. L. (1992). "Transition to shear-driven turbulence in Couette-Taylor flow," *Physical Review A* 46(10), 6390-6405.
- Maynard, S. T. (1990). "Velocities induced by commercial navigation," Technical Report HL-90-15, U.S. Army Engineer Waterways Experiment Station, Vicksburg, MS.
- _____. (1996). "Return velocity and drawdown in navigable waterways," Technical Report HL-96-7, U.S. Army Engineer Waterways Experiment Station, Vicksburg, MS.
- _____. "Physical forces near commercial tows," (Technical Report in preparation), U.S. Army Engineer Research and Development Center, Vicksburg, MS.
- Maynard, S. T., and Martin, S. K. (1997). "Interim report for the Upper Mississippi River - Illinois Waterway System navigation study, physical forces study, Kampsville, Illinois Waterway," ENV Report 3, U.S. Army Engineer Districts, Rock Island, St. Louis, and St. Paul.
- Morgan R. P., Ulanowicz, R. E., Rasin, V. J., Jr, Noe, L. A., and Gray, G. B. (1976). "Effects of shear on eggs and larvae of striped Bass, *Morone saxatilis*, and white perch, *M. Americana*," Natural Resources Institute, Chesapeake Biological Laboratory, University of Maryland, Center for Environmental and Estuarine Studies, *Transactions of the American Fisheries Society* (1), 149-154.

Schlichting, H. (1968). "Boundary-layer theory." 6th ed., McGraw Hill, New York.

U.S. Army Engineer Districts, St. Paul, Rock Island, and St. Louis. (1994). "Upper Mississippi River - Illinois Waterway System navigation study," Baseline Initial Project Management Plan, St Paul, MN, Rock Island, IL, and St Louis, MO.

REPORT DOCUMENTATION PAGE

Form Approved
OMB No. 0704-0188

Public reporting burden for this collection of information is estimated to average 1 hour per response, including the time for reviewing instructions, searching existing data sources, gathering and maintaining the data needed, and completing and reviewing the collection of information. Send comments regarding this burden estimate or any other aspect of this collection of information, including suggestions for reducing this burden, to Washington Headquarters Services, Directorate for Information Operations and Reports, 1215 Jefferson Davis Highway, Suite 1204, Arlington, VA 22202-4302, and to the Office of Management and Budget, Paperwork Reduction Project (0704-0188), Washington, DC 20503.

1. AGENCY USE ONLY (Leave blank)	2. REPORT DATE February 2000	3. REPORT TYPE AND DATES COVERED Interim report	
4. TITLE AND SUBTITLE Shear Stress on Shallow-Draft Barge Hulls			5. FUNDING NUMBERS
6. AUTHOR(S) Stephen T. Maynard			
7. PERFORMING ORGANIZATION NAME(S) AND ADDRESS(ES) U.S. Army Engineer Research and Development Center 3909 Halls Ferry Road Vicksburg, MS 39180-6199			8. PERFORMING ORGANIZATION REPORT NUMBER
9. SPONSORING/MONITORING AGENCY NAME(S) AND ADDRESS(ES) See reverse.			10. SPONSORING/MONITORING AGENCY REPORT NUMBER ENV Report 24
11. SUPPLEMENTARY NOTES			
12a. DISTRIBUTION/AVAILABILITY STATEMENT Approved for public release; distribution is unlimited.			12b. DISTRIBUTION CODE
13. ABSTRACT (Maximum 200 words) <p>The Upper Mississippi River-Illinois Waterway System (UMR-IWWS) Navigation Study evaluates the justification of additional lockage capacity at sites on the UMR-IWWS while maintaining the social and environmental qualities of the river system. The system navigation study is implemented by the Initial Project Management Plan (IPMP) outlined in the "Upper Mississippi River-Illinois Waterway System Navigation Study," (U.S. Army Corps of Engineers (USACE) 1994). The IPMP outlines Engineering, Economic, Environmental, and Public Involvement Plans.</p> <p>Physical forces in the region near and beneath commercial tows occur because of the propeller jet and the displacement of water by the hull of the vessel. Physical forces are quantified in terms of the changes in pressure, velocity, and shear stress and are used to determine substrate scour, sediment resuspension, and effects on aquatic organisms.</p> <p>This study of forces near and beneath commercial tows is conducted in a physical model. The reason for this is that field measurements beneath a vessel are difficult to obtain because some of the primary tows of interest are operating in shallow water with as little as a 0.6-m clearance beneath the tow. In addition, propeller jet bottom velocities can exceed 4 m/sec. Operation of velocity meters or other measuring devices in such an environment is quite difficult. The difficulty of obtaining field data means that verification data for the physical model is lacking. The approach used herein is to</p> <p style="text-align: right;">(Continued)</p>			
14. SUBJECT TERMS			15. NUMBER OF PAGES 32
			16. PRICE CODE
17. SECURITY CLASSIFICATION OF REPORT UNCLASSIFIED	18. SECURITY CLASSIFICATION OF THIS PAGE UNCLASSIFIED	19. SECURITY CLASSIFICATION OF ABSTRACT	20. LIMITATION OF ABSTRACT

9. (Concluded).

U.S. Army Engineer District, Rock Island, Clock Tower Building, P.O. Box 2004, Rock Island, IL 61204-2004
U.S. Army Engineer District, St. Louis, 1222 Spruce Street, St. Louis, MO 63103-2833
U.S. Army Engineer District, St. Paul, Army Corps of Engineers Centre, 190 5th Street East, St. Paul, MN 55101-1638

13. (Concluded).

use a large physical model to minimize scale effects. Propeller jets, a main emphasis of this study, are operated at speeds where the thrust coefficients are independent of Reynold's number, suggesting similarity with the prototype.

The results presented herein for the physical forces near commercial tows focus on the design tow using the UMR-IWWS. The design tow is a three-wide by five-long barge tow, loaded to about 2.74 m and pushed by a twin-screw towboat with open-wheel or Kort nozzle propellers, typically about 2.74 m in diameter. These data are from experiments in a 1:25-scale model channel, barges, and towboat that has operating propellers, rudders, and open-wheel or Kort nozzle propellers.

The following parameters were measured in the model:

- a. Channel bottom pressure under moving tow.
- b. Near-bed velocity and bed shear stress changes under the barges of a moving tow.
- c. Near-bed velocity and bed shear stress changes in the stern region from the propeller jet for a stationary tow and from the combined effects of the propeller jet and the wake flow for a moving tow.

Analytical/empirical methods were developed to describe near-bed velocity and shear stress as a function of tow parameters.